Journal of Plant Physiology 249 (2020) 153166

Contents lists available at ScienceDirect

Journal of Plant Physiology

journal homepage: www.elsevier.com/locate/jplph

Functional characterisation and *in silico* modelling of *MdPSY2* variants and *MdPSY5* phytoene synthases from *Malus domestica*

Ariel Cerda[a,1], Juan C. Moreno[b,1], Daniel Acosta[a], Francisca Godoy[a], Juan Carlos Cáceres[a], Ricardo Cabrera[a], Claudia Stange[a,*]

[a] Departamento de Biología, Facultad de Ciencias, Universidad de Chile, Las Palmeras 3425, Casilla 653 Ñuñoa, Santiago, Chile
[b] Max-Planck-Institut für Molekulare Pflanzenphysiologie, Am Mühlenberg1 D-14476, Potsdam-Golm, Germany

ARTICLE INFO

Keywords:
Carotenoids
Malus domestica cv. 'Fuji'
Phytoene synthase
Heterologous complementation
In silico modelling

ABSTRACT

Carotenoids are plastid isoprenoid pigments that play critical roles in light harvesting, photoprotection, and phytohormone biosynthesis. They are also vitamin-A precursors and antioxidant molecules important for human nutrition. Apples (*e.g. Malus x domestica* Borkh), one of the most widely consumed fruits with high nutrient levels, have a very low carotenoid concentration in flesh, compared with other fruits and vegetables. This could be explained by a deficiency in carotenoid synthesis/accumulation and/or accelerated degradation. We analysed the contribution of *M. domestica* cv. 'Fuji' phytoene synthase (PSY) in the biosynthesis of carotenoids and determined that among four *MdPSY* genes present in the organism, *MdPSY2* and *MdPSY5* are highly expressed in leaves and during fruit ripening in line with an increment in carotenoid content in fruits. Furthermore, two representative polymorphic *MdPSY2* variants were found, one with a Tyr358Phe substitution (*Md*PSY2_*F*) and the other that additionally has a six-amino-acid deletion in the signal peptide (*Md*PSY2_*CG*). *Md*PSY2, *Md*PSY5, *Md*PSY2_F and *Md*PSY2_CG are all localised in plastids. Interestingly, the polymorphic *Md*PSY2_F and *Md*PSY2_CG variants show lower enzymatic activity than the wild-type form in a heterologous complementation assay, which could be attributed to the Tyr358Phe substitution close to the active-site pocket, as was suggested by 3-D modelling analysis. The presence of polymorphic *Md*PSY2 variants with lower enzymatic activity could be partially responsible for the low carotenoid content in Fuji apple fruits.

1. Introduction

Carotenoids are important isoprenoid compounds in plant metabolism. They are synthesised in plastids (*e.g.* chloroplasts) and act as accessory pigments during photosynthesis and protect cells from photo-oxidative damage (Kromdijk et al., 2016; Nisar et al., 2015). The oxidative cleavage of these compounds gives rise to several apocarotenoids, such as the phytohormones abscisic acid and strigolactones (Beltran and Stange, 2016). In fruits and flowers, they accumulate in specialised plastids (*e.g.* chromoplasts) providing yellow, orange and red colours, and act as attractants for pollinators and seed dispersal agents (Rosas-Saavedra and Stange, 2016). In mammals, carotenoids are the main source of vitamin A and have powerful antioxidant properties (Fraser and Bramley, 2004; Rao and Rao, 2007; Ruiz-Sola and Rodriguez-Concepcion, 2012).

Carotenoid synthesis in plants is regulated at 3 different levels: (1) the transcription of genes involved in carotenoid biosynthesis and degradation, (2) the activity and stability of producing enzymes, and (3) the presence of carotenoid storage structures in plastids (Li et al., 2016). Thus, carotenoid abundance is the overall result of metabolic flux regulation, combining key enzymes in biosynthesis (phytoene synthase/PSY), degradation (carotenoid cleavage dioxygenase/CCDs) and protein stability (orange protein/OR). For instance, OR stabilises PSY, improving carotenoid accumulation and storage in plastoglobuli (Li et al., 2016).

The carotenoid biosynthetic pathway has been well described (Fraser and Bramley, 2004; Ruiz-Sola and Rodriguez-Concepcion, 2012) and various reports have concluded that the key point of carotenoid flux regulation is the first step in the pathway, catalysed by PSY (Lois et al., 2000; Rodriguez-Villalon et al., 2009; von Lintig et al., 1997) (Fig. 1). In *Arabidopsis thaliana*, PSY is encoded by a single gene copy. However in many crops such as *Oryza sativa* (rice) (Welsch et al., 2008), *Cucumis melo* (melon) (Qin et al., 2011), *Manihot esculenta* (cassava) (Arango et al., 2010), *Daucus carota* (carrot) (Just et al.,

* Corresponding author.
E-mail address: cstange@uchile.cl (C. Stange).
[1] These authors contributed equally to this work.

https://doi.org/10.1016/j.jplph.2020.153166
Received 11 July 2019; Received in revised form 23 March 2020; Accepted 26 March 2020
Available online 25 April 2020

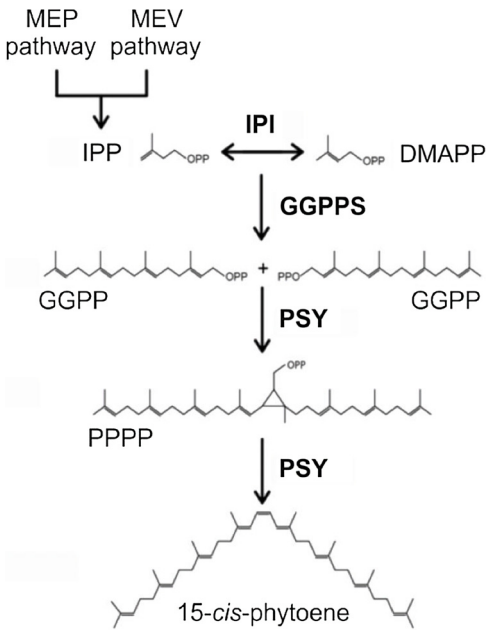

Fig. 1. Biosynthesis of 15-*cis*-phytoene. All the steps involved in the conversion of isopentenyl pyrophosphate (IPP) into 15-*cis*-phytoene are shown. DMAPP: dimethylallylpyrophosphate; IPI: isopentenyl diphosphate isomerase; GGPPS: geranyl geranyl diphosphate synthase; GGPP: geranyl geranyl diphosphate; PSY: phytoene synthase; PPPP, pre-phytoene diphosphate.

2007), *Solanum lycopersicum* (tomato) (Fraser et al., 1999) and *Zea mays* (maize) (Welsch et al., 2008), it is present as a small gene family exhibiting organ or environmental stimuli specificity.

Although *PSY* expression generally correlates with an increment in carotenoid content in different fruits (Fraser et al., 1999; Giovannoni, 2001; Kato et al., 2004; Ronen et al., 1999; Tao et al., 2007), its functionality also depends on the levels of enzymatic activity. PSY, along with isopentenyl isomerase (IPI) and geranyl geranyl pyrophosphate synthase (GGPPS) form a soluble multienzyme complex, whose activity depends on its association with the thylakoid membrane (Fraser and Bramley, 2004; Fraser et al., 2000; Li et al., 2008; Ruiz-Sola and Rodriguez-Concepcion, 2012; Schledz et al., 1996). In *A. thaliana* and *Sinapis alba*, PSY activity increases when plants are exposed to light (Welsch et al., 2000); nevertheless the most relevant role of PSY has been shown in sink organs where high levels of carotenoids are accumulated in crystalline structures (Maass et al., 2009). Coloured varieties of *Z. mays* and *M. esculenta* accumulate carotenoids due to the presence of functional PSY alleles which differ in one nucleotide from the wild-type allele of white varieties (Shumskaya et al., 2012; Welsch et al., 2010). The T257P mutation in *ZmPSY2* affects its localisation, producing changes in the plastoglobuli structure, affecting the carotenoid content in maize endosperm (Shumskaya et al., 2012). Similarly, *M. esculenta* presents single nucleotide polymorphisms (SNPs) in *MePSY2*, defining two alleles for the yellow cultivar (R174 T and A191D) and one homonymous SNP to the white one (Welsch et al., 2010) in which the PSY2 A191D mutant showed the highest enzymatic activity (Welsch et al., 2010). In *S. lycopersicum* two point mutations in the trans isoprenyl diphosphate synthase domain of *SlPSY1* were identified (Gady et al., 2012). The W180* mutation produces a knock-out allele resulting in fruits with deeper yellow flesh colour at the ripe stage, while the P192L allele produces red fruits at the ripe stage. The P192L allele shows an additional alpha helix around the mutation position which could be the cause of the reduced enzymatic activity (Gady et al., 2012).

Apples (*Malus x domestica* Borkh) are one of the most widely consumed fruits, and are rich in nutritional metabolites such as fibre, flavonoids, and vitamin C. Most of the cultivated apple varieties are diploids (2n = 34), auto-incompatible and have a juvenile stage of 5–10 years. The apple genome is available and has a size of approximately 750 Mb (Velasco et al., 2010). Carotenoids that are present in apple skin reach more than 6.6 μg/g fresh weight in commercial 'Royal Gala', contributing to fruit colouration and attractiveness (Ampomah-Dwamena et al., 2012). However, these commercial apple varieties have white or pale-yellow flesh with reduced carotenoid content (< 2 μg/g of fresh weight) (Ampomah-Dwamena et al., 2012). Currently there is no clear evidence that can allow us to determine whether the low carotenoid content in apple fruits is due to reduced biosynthesis, deficient accumulation, and/or an increase in metabolic degradation. Z-carotene isomerase (ZISO) and carotenoid isomerase (CRTISO) have been proposed as potential rate-limiting steps in apple carotenoid synthesis, both in pigmented and commercial non-pigmented cultivars, by employing expression analysis of genes involved in carotenoid synthesis and degradation (Ampomah-Dwamena et al., 2012). However, this has not been confirmed at the functional level (Ampomah-Dwamena et al., 2012).

In *M. domestica*, six *PSY* genes have been described, but only four could be amplified (Ampomah-Dwamena et al., 2012). Expression analysis of the four *MdPSY* genes showed very low expression in the flesh of the red cultivar (Aotea) and higher expression in pale yellow cultivars (M9 and Royal Gala), suggesting no direct correlation with carotenoid accumulation (Velasco et al., 2010). Comparing *MdPSY1* and *MdPSY2* expression in 'Granny Smith' and 'Royal Gala' apple cultivars, *MdPSY2* showed a higher expression level in fruit skin and flesh, and other vegetative tissues (Ampomah-Dwamena et al., 2015), and both showed activity in a complementation assay and had a chloroplastidial localisation (Ampomah-Dwamena et al., 2015). Nevertheless, no specific expression analysis studies have been performed in order to compare the expression of each of the four *MdPSY* genes in fruit flesh.

In this work, we conducted an *in silico* comparative analysis of *MdPSY1, MdPSY2, MdPSY3* and *MdPSY5* genes, and performed an expression analysis in leaves and fruits during three stages of ripening in the 'Fuji' cultivar. *MdPSY2* and *MdPSY5* were the most highly expressed genes in mature fruits, correlating with carotenoid abundance in flesh. For this reason, they were selected for further characterisation. During *MdPSY2* cloning, two representative polymorphic variants were found (named *MdPSY2_F* and *MdPSY2_CG*), and therefore included for further analysis. The *MdPSY2_F* allele presented a Tyr358Phe substitution while *MdPSY2_CG* had the same substitution and a deletion of 18 bp between the base pair 92 and 109 and a 121 G > A (G41S) mutation in the signal peptide. All *MdPSY2* variants and *MdPSY5* were localised in chloroplasts. Heterologous expression in *Escherichia coli* revealed that the enzymatic activity of wild type *MdPSY2* and *MdPSY5* is higher than that of the *MdPSY2_F* and *MdPSY2_CG* variants. A 3D model of *MdPSY2_F* suggests that the Tyr358Phe substitution may affect electrostatic interaction between surrounding residues that could explain the lower enzymatic activity of *MdPSY2_F* and *MdPSY2_CG*. The presence of the two polymorphic *MdPSY2* variants with lower enzymatic activity – a result of the Tyr358Phe substitution – could be in part responsible for the low carotenoid content in the flesh of Fuji apples.

2. Materials and methods

2.1. Sequence and phylogenetic analyses of the MdPSY gene family

The different nucleotide sequences of the *M. domestica PSY* gene family were obtained from the Genome Data base of Rosacea species (GDR) and the published sequence of the apple genome (Velasco et al., 2010) (S Text S1). In addition, the online Basic Local Alignment Search Tool (BLAST) was employed to align putative *PSY* nucleotide sequences with known *PSY* nucleotide sequences from other organisms (S Table S1). The gene structure was obtained from Expressed Sequence Tag (EST) information available in ESTIMA: Apple (Kumar et al., 2004) and

KEGG (http://www.genome.jp/dbget-bin/www_bget?gn: T03194). With this information, their genetic structure was determined (S Table S2). Amino acid sequence alignments were performed using the online tool Clustal Omega (https://www.ebi.ac.uk/Tools/msa/clustalo/), and edited using the Jalview program (Waterhouse et al., 2009) to compare the obtained sequences with known PSY proteins from other organisms (Fig. S1). A phylogenetic tree was built using MEGA version X (Kumar et al., 2018) with the neighbour joining algorithm performing 10,000 iterations ("pseudo replica") and selecting the most representative tree. Accession numbers of the PSY proteins from different organisms used to build the phylogenetic tree are shown in Table S3. *In silico* chloroplast transit peptide (cTP) prediction of apple PSY enzymes was performed using the ChloroP server (Table S4).

2.2. Plant material

Leaves and fruits from *M. domestica* cv. 'Fuji' Raku Raku were collected from different apple trees during the harvest season in Paine, Santiago, Chile (33.8126 °S, 70.7376 °W). Mature leaves similar in size, colour and shape were collected (three groups of three leaves each). In the case of the fruits, nine fruits (grouped in three fruits each) in three different developmental/ripening stages were selected (S1, S2, and S3). These developmental stages were chosen in accordance to the skin colour, days after full bloom (dafb) and hypanth starch content. S1, S2 and S3 stages correspond to 127, 168 and 211 dafb, respectively. A fruit of 127 dafb has reached its mature size but is still green and presents a predominant accumulation of starch, at 168 dafb, the fruit is at an intermediate ripening stage, showing initial flesh colouring and at 211 dafb, the 'Fuji' fruit reaches its full mature stage.

2.3. RNA extraction and qRT-PCR

A previously described protocol (Meisel et al., 2005), was used to extract RNA from 300 mg of three different group of leaves and from four grams of flesh (hypanthium) from each group of fruits by grinding in a pre-cooled mortar and pestle. Afterwards, 10 mL of pre-heated (65 °C) extraction buffer (CTAB 2%, PVP40 2% [PM, 40.000], EDTA 25 mM, NaCl 2 M, TrisHCl [pH 8.0] 100 mM, spermidine trihydrochlorate 0.05% and β-mercaptoethanol 2%) was added. The mixture was incubated for 30 min at 65 °C with agitation. Subsequently, 1 vol of chloroform:isoamyl alcohol (24:1) was added and centrifuged for 20 min at 12,000 g at 4 °C. One volume of LiCl 10 M was added to the aqueous phase and incubated overnight at 4 °C and centrifuged at 12,000 g for 30 min at 4 °C. The RNA was resuspended in 500 µL of RNAse-free water. One volume of chloroform:isoamyl alcohol (24:1) was added, centrifuged at 14,000 g for 10 min at 4 °C and washed with 75% ethanol. The RNA was dried and then resuspended in 20 µL of RNAse-free water and stored at −80 °C. Genomic DNA traces were eliminated by incubating for 20 min with DNase I. For cDNA synthesis, 7 µg of total DNA-free RNA was mixed with 1 mM of primer AP (Table S5) and Impron II reverse transcriptase (Promega). Quantitative RT-PCR (qRT) experiments were performed as described in (Fuentes et al., 2012) using a Stratagene Mx3000 P thermocycler, employing SYBR Green double strand DNA binding dye. Specific primers used to amplify the *MdPSYs, MdPDS* and *MdLCYBs* genes are shown in Table S5. *Actin, ubiquitin* and *18S* (primers in Table S5) were evaluated as normalisers; *actin* was selected after analysis by NormFinder (Andersen et al., 2004). Final data was obtained introducing fluorescence results in the equation: Ecarot ΔCP gene (Ct ubiq − Ct gene)/E ubiq ΔCP ref (Ct ubiq − Ct gene) (Pfaffl, 2001). Each qRT-PCR reaction was performed with three biological and three technical replicates. In all cases, the reaction specificities were tested with melting gradient dissociation curves and electrophoretic gels.

2.4. Pigment extraction and high-performance liquid chromatography (HPLC and RP-HPLC)

For pigment quantification, 4 g of flesh (hypanthium) from each of the three groups of fruits was ground in a pre-cooled mortar and pestle. Then, 20 mL of a hexane:acetone:ethanol (2:1:1) solution was added and transferred to a Falcon tube and incubated during two minutes with agitation in darkness at 4 °C, followed by a centrifugation step at 14,000 g for 10 min at 4 °C. Carotenoids were recovered from the upper phase and dried out using gaseous nitrogen. Afterwards, the pigments were resuspended in 400 µL of acetone for quantification. Each ripening state (S1–S3) was evaluated using three independent replicates. Carotenoids from *E. coli* BL21 complemented cells were extracted from 70 mL of liquid cultures as described in Moreno et al. (2013). The extraction process was performed avoiding light and using ice to maintain carotenoid integrity. Total carotenoids and chlorophylls were measured by spectrophotometry at 474 nm (carotenoids), 645/662 nm (chlorophylls) and 520/750 nm (normalisation). Specific carotenoids were quantified by a Shimadzu HPLC (LC-10AT) with a diode array, and data analysis was carried out using previously described equations (Lichtenthaler and Buschmann, 2001). All data is shown as µg/g of dry weight. The quantified pigments were isolated by HPLC using a MultoHigh 100 RP 18 − 5µ (150 × 4.6 mm) column, using a mobile phase of acetonitrile:methanol:isopropanol (85:10:5 v/v) with a flow rate of 1.5 mL/min during 1 h at room temperature in isocratic conditions. Carotenoids were identified according to their absorption spectra, retention time and comparison with specific pigment standards.

2.5. Gene amplification and vector construction

The full-length coding sequences of *MdPSY2* (1184 bp) and *MdPSY5* (1284 bp) genes were amplified using *M. domestica* cDNA from fruits as template with specific primers (Table S5) and Pfu DNA polymerase (New England Biolabs). The amplified fragments were cloned into pCR8/GW/TOPO (Invitrogen) following the manufacturer's instructions and positive clones were sequenced by Macrogen Corp. (USA). Three clones for pCR8/*MdPSY5* were sequenced showing 100% identity between them, while for pCR8/*MdPSY2*, three different sequences were obtained. Therefore, 5 additional pCR8/*MdPSY2* clones were sequenced, obtaining, from a total of eight clones, three with the expected (wild type) sequence, two with a Y358 F substitution at the C-terminal region (*MdPSY2*_F), which is also found in the apple genome, and three with both the Y358 F substitution, a 121 G > A (G41S) silent mutation and a deletion of 18 nucleotides in the predicted transit peptide region (*MdPSY2*_CG). All clones were sequenced twice.

2.6. Subcellular localisation

The full-length *MdPSY2, MdPSY2*_F, *MdPSY2*_CG and *MdPSY5* coding sequences were amplified without the stop codon from the previously sequenced pCR8/*MdPSYs* clones, subcloned into pCR8/GW/TOPO (Invitrogen) and thereafter recombined into the binary vector pMDC85 (Curtis and Grossniklaus, 2003) obtaining the chimeric proteins *Md*PSYs:GFP under the control of the 35SCaMV promoter. As a control, the plastidial enzyme *At*DXR:GFP (Carretero-Paulet et al., 2002) and the nuclear cofactor *At*PAR1:GFP (Bou-Torrent et al., 2015) were included. The constructs were transiently expressed in 2-month-old leaves from *Nicotiana tabacum* plants by agroinfiltration using the protocol described by Moreno et al. (2013). Samples were visualised in a confocal LSM510 microscope 6 days post infiltration. The GFP signal was measured at 40X and processed with LSM5 Image Browser.

2.7. Heterologous complementation in E. coli

The pCR8/*MdPSY2* (three versions) and pCR8/*MdPSY5* constructs were digested with BamHI and SalI and cloned into the expression

vector pET28a (previously digested with the same enzymes) generating the expression vectors pET28a/*MdPSY2*_F, pET28a/*MdPSY2*_CG, pET28a/*MdPSY2* and pET28a/*MdPSY*5 (Table S6). Functional assays were carried out in the *E. coli* BL21 gold strain transformed with the pDS1B or pDS1BΔcrtB plasmids. pDS1B carries the carotenogenic genes of *Erwinia uredovora* required for β-carotene synthesis (Sievers et al., 2011). The pDS1BΔcrtB vector has a mutation in the crtB (*PSY*) gene, which blocks the production of β-carotene (Niklitschek et al., 2008). This mutant strain was transformed with pET28a/*MdPSY2*_F, pET28a/*MdPSY2*_CG, pET28a/*MdPSY2*, pET28a/*MdPSY*5 and the empty pET28a vector (EV) as control. The transformed colonies were selected in LB medium supplemented with kanamycin (100 μg/mL) and chloramphenicol (34 μg/mL), after an incubation of 48 h at 28 °C. An overnight liquid culture of the mutant strain transformed with each vector was used to inoculate 5 mL of LB medium supplemented with the aforementioned antibiotics and incubated with agitation for 16 h at 37 °C. Subsequently, 2 mL of the overnight culture was used to inoculate 200 mL of LB medium with the selective antibiotics. When the culture reached OD600nm: 0.6, 1 mM of IPTG (isopropyl β-D-thiogalactoside) was added to half of the culture to induce the expression of the gene, and the other half was used as control. All the assays were performed in triplicate and in darkness, in order to maximise carotenoid production. For protein extraction and immunoblot analysis, total proteins were extracted from BL21 strains complemented with pET28a/*MdPSY2*_F, pET28a/*MdPSY2*_CG, pET28a/*MdPSY2*, pET28a/*MdPSY*5 and the empty pET28a vector (EV), following the manufacturer´s instructions (Thermo Scientific). Total soluble proteins were quantified by the Bradford method (Bradford 1976) and 30 μg were resolved by 10% SDS-PAGE and transferred to a nitrocellulose membrane using the Transfer System RTA Transfer Packs kit (BioRad) and the TransBlot system (BioRad) at 400 mA, 4 °C for 10 min. Membranes were blocked for 3 h in TBS-T (20 mM Tris − HCl pH 7.5, 140 mM NaCl, 0.1% 159 Tween-20) and 5% non-fat milk, and then washed 3 times during 10 min with TBS-T. Protein transfer was verified by Ponceau and Coomassie blue staining. For immunoblotting, the membrane was incubated in rabbit polyclonal anti-PSY antisera primary antibody (1:1000; AS16 3991 Agrisera) for 1 h, washed 3 times for 10 min with TBS-T and then incubated with anti-mouse IgG alkaline phosphatase (1:10000; 028M4755V Sigma) as the secondary antibody at 37 °C for 1 h. Antibody binding was detected with nitro-blue tetrazolium chloride and 5-bromo-4-chloro-3′-indolyphosphate p-toluidine salt and visualised by UVITEC Cambridge (Biomolecular Imaging- Alliance © Software) and using the Image Studio Lite™ Software (LI-COR ® Bio). Immunoblot was performed three times.

2.8. D-modelling of MdPSY5, MdPSY2 and MdPSY2_F proteins

Homology modelling was performed following the schematic workflow shown in Fig. S2. In brief, three templates with known crystallographic structures were identified in the Protein Data Bank (PDB) (www.rcsb.org). These three structures were the squalene synthase from *Alicyclobacillus acidocaldarius* (PDBid: 4HD1), dehydro squalene synthase from *Staphylococcus aureus* (PDBid:2ZCO), and squalene synthase from *Homo sapiens* (PDBid:3VJ8). The sequence identity of *Md*PSY2 was 28% with 4HD1, 25% with 2ZCO and 22% with 3VJ8, while for *Md*PSY5, the identity was 29% with 4HD1, 26% with 2ZCO and 20% with 3VJ8. A multiple sequence alignment was built using ClustalO (www.ebi.ac.uk/Tools/msa/clustalo/) (Sievers et al., 2011) excluding the N-terminal region corresponding to the transit peptide. With this information, protein models were generated using the software MODELLER (v. 9.13; https://salilab.org/modeller/). These models were refined using the 3Drefine (http://sysbio.rnet.missouri.edu/3Drefine) server, which optimises hydrogen bonds and performs energy minimisation modifying parameters related to torsion, angle and turn of bonds. In addition, the KoBaMIN (http://csb.stanford.edu/kobamin) server was used to perform a potential energy minimisation. Refined models were evaluated using the server ModFOLD4 (www.reading.ac.uk/bioinf/ModFOLD) which selects the best model by evaluating structural features and energy profiles from all the models generated, followed by clustering approximation (www.ncbi.nlm.nih.gov/pmc/articles/PMC3692122/). One model was selected for each protein according to the highest score obtained. The 3D-1D energy profile of the best models was calculated using the Verify3D server and compared to their templates. All protein structures were visualised using VMD (www.ks.uiuc.edu/Research/vmd/ (Humphrey et al., 1996)) and structural superpositions were performed using the Multiseq software (https://doi.org/10.1186/1471-2105-7-382).

3. Results

3.1. In silico analysis of Malus domestica PSY genes

Gene models of twelve putative *PSY* genes of *M. domestica* were obtained from the GDR database and from the apple genome (Table S1). The sequences of most of these genes lack the common exon/intron patterns or show poor contig alignment. In order to strengthen our analysis, we used EST (ESTIMA: Apple) and KEGG databases, finding four putative genes (Table S2) which were named according to Ampomah-Dwamena et al. (2015). When we compared our results with those of Ampomah-Dwamena et al. (2015), we discovered that *MdPSY5* was absent from their work, as it is present in current EST databases but not in the apple EST libraries (Newcomb et al., 2006) used in their study. This highlights the importance of using a larger database, such as ESTIMA. These genes contain the ORF and 5′ and/or 3′ UTR regions. With this information, we built the gene structures for four different *PSY* genes from apple: *MdPSY1*, *MdPSY2*, *MdPSY3* and *MdPSY5* (Fig. 2 a). All contain 5 − 6 exons, and their structures correspond to those previously reported in *S. lycopersicum*, *Capsicum annuum*, *Hordeum vulgare* and *Z. mays*, as well as *M. domestica* (Ampomah-Dwamena et al., 2015; Fu et al., 2010; Guzman et al., 2010; Mann et al., 1994; Rodriguez-Suarez et al., 2011). Moreover, these four *PSY*s possess the functional domain of trans-isoprenyl diphosphate synthases that catalyses the condensation of 1′-1 of two isoprenyl diphosphates, of 15 or 20 carbons (Trans_IPPS-HH, NCBI – Conserved Domains). In addition, amino acid sequence alignments including six other members of the plant PSY family, reveal that *Md*PSY1, *Md*PSY2, *Md*PSY3 and *Md*PSY5 (Fig. S1) harbour the main functional motifs of a PSY enzyme (Gu et al., 1998; Pandit et al., 2000; Tansey and Shechter, 2000). As in many cases, the evolutionary origin may reveal the function or specificity of PSY enzymes (Cunningham et al., 1996; Alquezar et al., 2009; Ronen et al., 2000; Hirschberg, 2001). Therefore, we performed phylogenetic analysis using the neighbour-joining method with PSY sequences from bacteria, green algae and plants (Fig. 2b; Table S3). *Md*PSY5 grouped in a clade with PSYs from dicots such as tomato (*Sl*PSY1 and *Sl*PSY2), Arabidopsis (*At*PSY), carrot (*Dc*PSY2), cassava (*MePSY1* and *MePSY2*), nappa cabbage (*Br*PSY1), soybean (*Gm*PSY1) and sweet oranges (*Cs*PSY1). *Md*PSY1 and *Md*PSY2, which share 93.7% sequence identity, grouped in a clade containing both dicots (carrot *Dc*PSY1 and soybean *Gm*PSY2A/PSY2B) and monocots (maize *Zm*PSY2, rice *Os*PSY2 and Brachypodium *Bd*PSY2). Finally, *Md*PSY3 is found distant from the other clades, which could be related to a group of 13 additional amino acids which are not present in the other PSYs (Fig. S1). Interestingly, *Md*PSY3 belongs to a recently described group consisting exclusively of dicot species, which is clearly distinguishable from the monocot PSY3 group. While the latter is related to ABA induced by abiotic stress, dicot PSY3s could be linked to root-specific expression during nutrient stress conditions (Walter et al., 2015).

3.2. Carotenoid composition and gene expression in fruits of Malus domestica cv. 'Fuji'

M. domestica cv. 'Fuji' Raku Raku was used in this study because it is

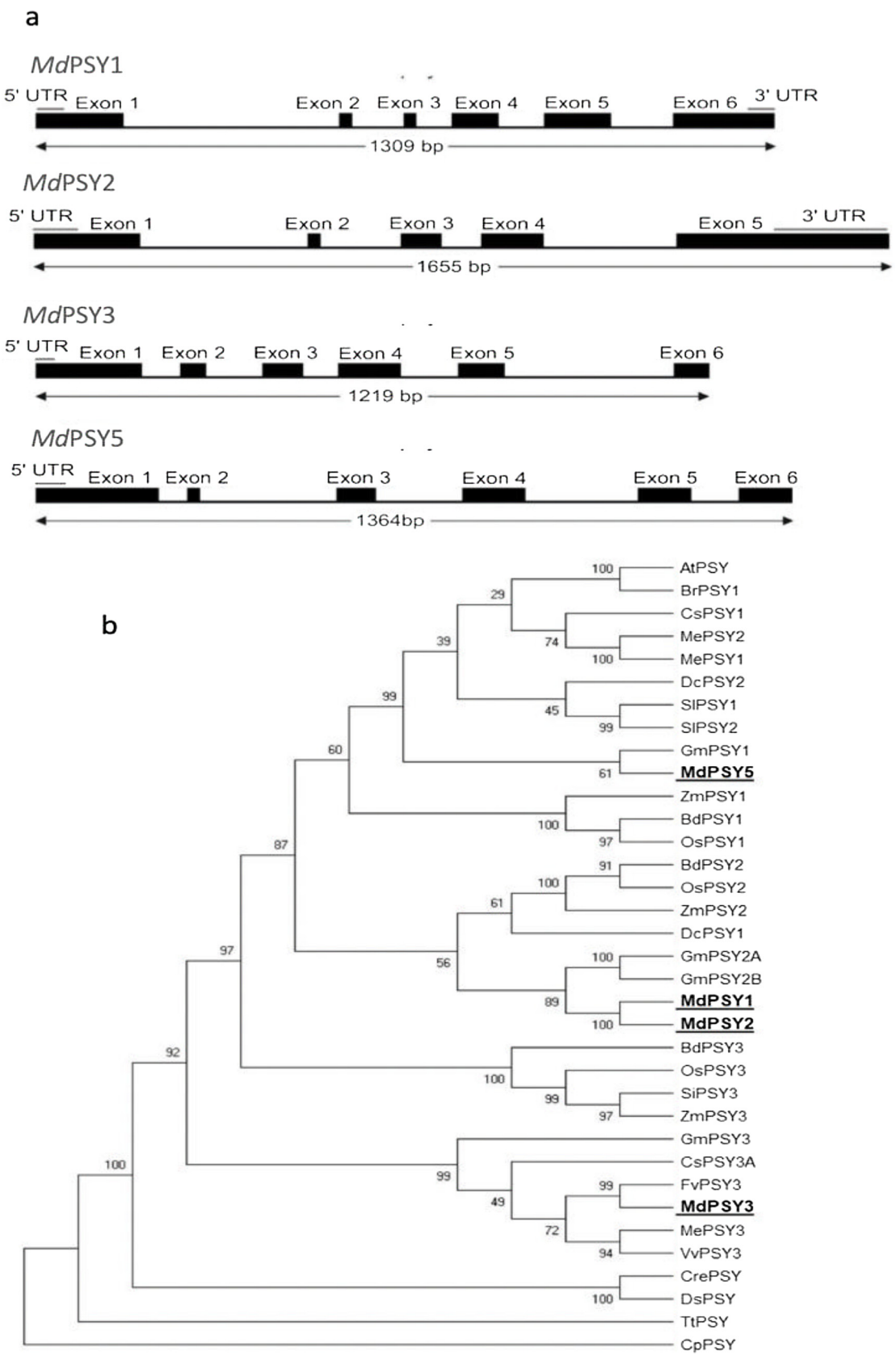

Fig. 2. Gene structure and phylogenetic analysis of *MdPSY3*, *MdPSY2*, *MdPSY5* and *MdPSY1*. **(**a) Gene structure of *MdPSY* genes assembled from EST data (KEGG and ESTIMA: Apple; see Materials and Methods). Probable exons are shown as black boxes and untranslatable regions (UTR) as grey lines. The sizes of the predicted genes are indicated below each gene structure. (b) Phylogenetic tree showing the phylogeny of *Md*PSY and other PSY enzymes from plants, green algae and bacteria. The phylogenetic tree was built using the neighbour-joining method based on 10,000 pseudo replicas of bootstrap. Numbers adjacent to branches are bootstrap values supporting this tree (see Materials and Methods). *Cp*PSY from *Candidatus pelagibacter* (YP_265548.1) and *Tt*PSY from *Thermus thermophilus* (AEG34638.1) were used for rooting. The species and Genbank codes used to construct the phylogenetic tree are shown in Table S3. (For interpretation of the references to colour in this figure legend, the reader is referred to the web version of this article.)

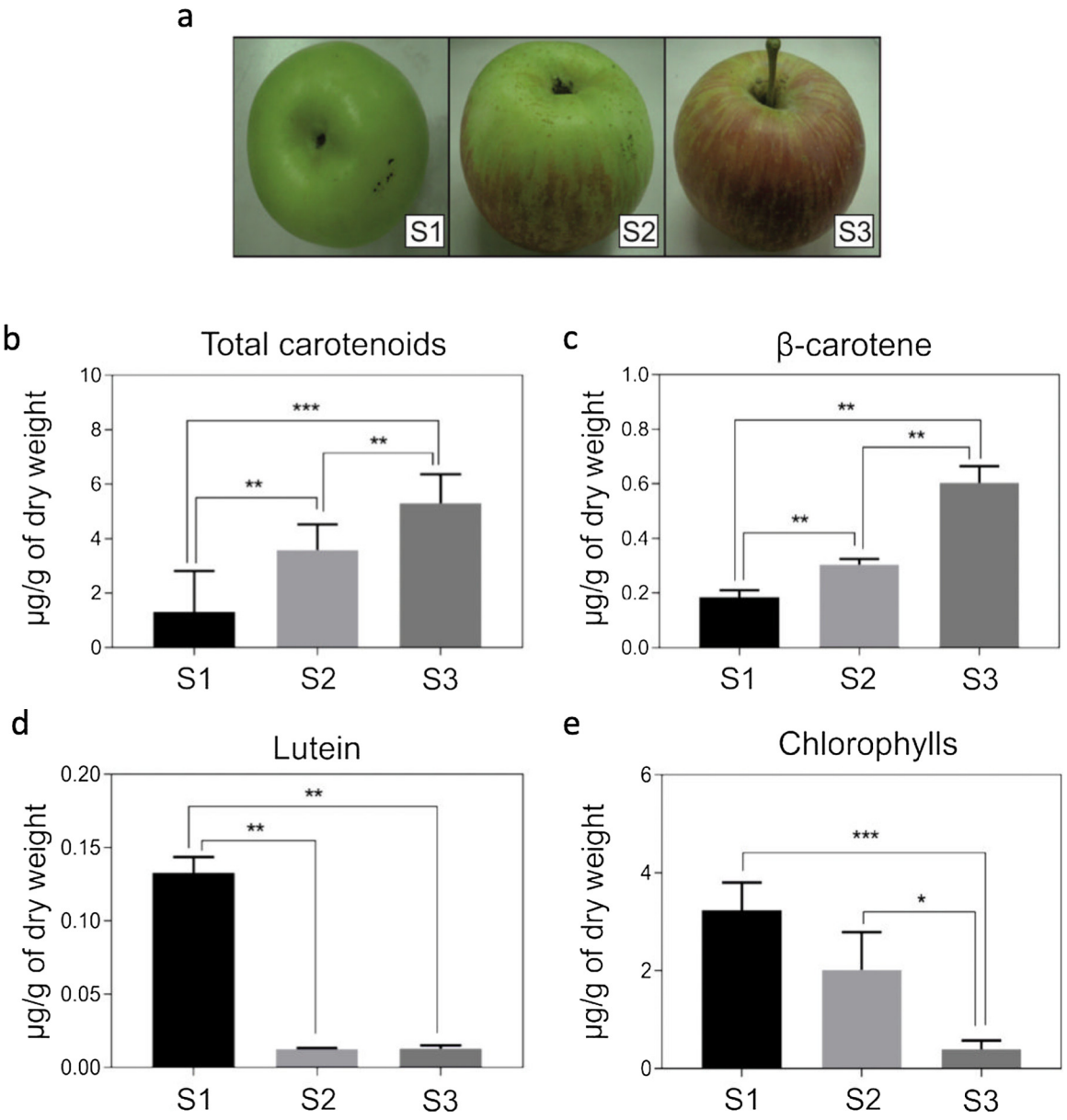

Fig. 3. Pigment quantification in *Malus domestica* var 'Fuji' fruit ripening stages. Composition and quantity of pigments during apple ripening was analysed by spectrophotometry and HPLC. (a) Three developmental stages were chosen in accordance to the skin colour, days after full bloom (dafb) and hypanth starch content. S1 (green), S2 (intermediate ripening stage) and S3 (full mature stage) stages correspond to 127, 168 and 211 dafb, respectively. (b) Total carotenoid content (carotenes and xanthophylls). (c) β-carotene content. (d) Lutein content. (e) Chlorophyll content (chlorophyll *a* and chlorophyll b). The values obtained for each pigment correspond to samples comprising three different fruits ($n = 3$) performed in triplicate. A non-paired two tailed Student *t*-test was performed to determine significant differences between samples. *: $p < 0.05$; **: $p < 0.01$; *** $p < 0.001$. (For interpretation of the references to colour in this figure legend, the reader is referred to the web version of this article.)

one of the four most important commercial varieties in Chile (www.odepa.gob.cl/). To gain insights into carotenoid metabolism in 'Fuji' apple fruits, we determined total carotenoid, β-carotene, lutein and chlorophyll composition in the flesh of fruits during three ripening stages: S1 (127 dafb), S2 (168 dafb) and S3 (211 dafb) (Fig. 3a). Total carotenoid (carotenoids and xanthophylls) content correlates positively with fruit ripening, increasing from 1 − 2 µg/g d.w. in S1 to 5 − 6 µg/g d.w. in S3 (Fig. 3b). The same pattern was observed for β-carotene with an increase from 0.18 µg/g d.w. in S1 to 0.65 µg/g d.w. in S3 (Fig. 3c). As expected, a negative correlation with fruit ripening was observed for lutein with a reduction from 0.14 µg/g d.w. in S1 to < 0.02 µg/g d.w. in S3 (Fig. 3d), and chlorophyll which fell from 3.5 µg/g d.w. in S1 to 0.4 µg/g d.w. in S3 (Fig. 3e). As previously reported (Fuentes et al., 2012; Hirschberg, 2001; Ruiz-Sola and Rodriguez-Concepcion, 2012), carotenoid accumulation is generally regulated at the transcriptional level of carotenogenic genes. Therefore, in order to evaluate whether carotenoid content correlates with the expression level of carotenogenic genes involved in the synthesis of β-carotene, we evaluated the expression pattern of *MdPSYs*, *MdPDS* and *MdLCYBs* genes from *M. domestica* cv. 'Fuji' Raku Raku in leaves and in the flesh of fruits in different ripening stages. *MdPSY2*, *MdPSY3* and *MdLCYB2* show fruit-specific expression in mature apple fruits (211 dafb, S3; Fig. 4a), while *MdPSY1*, *MdPSY5* and *MdLCYB1* are preferably expressed in leaves (Fig. 4a). Interestingly, the expression level of *MdPSY2* and *MdPSY5* is around 50-fold higher than that of other paralog genes. In the case of fruit ripening, the expression of *MdPSY3* is slightly induced in the flesh of mature fruits, *MdPSY2* expression drops 5-fold from S1 to S3, *MdPSY5* expression is induced 2.3-fold from S1 to S3 and *MdPSY1* is

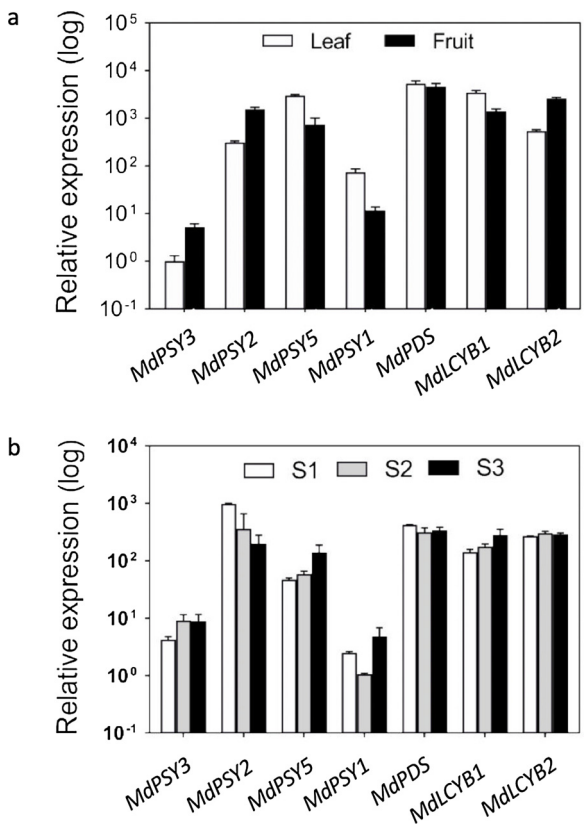

Fig. 4. Relative expression analysis of *MdPSY3*, *MdPSY2*, *MdPSY5* and *MdPSY1* in leaves and during *Malus domestica* var 'Fuji' fruit ripening. (a) Expression of *MdPSY3, MdPSY2, MdPSY5, MdPSY1, MdPDS, MdLCYB1* and *MdLCYB2* was determined by qRT-PCR in leaves and mature *M. domestica* cv. 'Fuji' Raku Raku fruits (S3, 211 dafb). (b) Expression of *MdPSY3, MdPSY2, MdPSY5, MdPSY1, MdPDS, MdLCYB1* and *MdLCYB2* genes was determined by qRT-PCR in S1 (127 dafb), S2 (168 dafb) and S3 (211 dafb) ripening stages. Each value in (a) and (b) corresponds to the average of three biological replicates and three technical replicates ($n = 9$). Actin was used as the normaliser gene and transcript abundance of *MdPSY1* was used as calibrator. A non-paired two tailed Student *t*-test was performed to determine significant differences between samples. *: $p < 0.05$; **: $p < 0.01$; *** $p < 0.001$.

also slightly induced at the mature stage. In addition, *MdPDS, MdLCYB1* and *MdLCYB2* showed no significant changes in transcript abundance in the three ripening stages (Fig. 4b). Interestingly, the expression level of *MdPSY2* and *MdPSY5* is around 100-fold higher than those of *MdPSY1* and *MdPSY3* (Fig. 4b). Thus, considering that *MdPSY5* presents relatively high transcript abundance in the flesh of mature fruits, and that its expression correlates with fruit maturation and carotenoid accumulation, we selected this gene for further studies. In addition, we included *MdPSY2* due to its high expression level in flesh and its fruit-specific expression.

Subcellular localisation and heterologous complementation of *Md*PSY2 and *Md*PSY5 proteins from *M. domestica* cv. 'Fuji'

In order to provide functional information on *MdPSY2* and *MdPSY5*, we performed subcellular localisation experiments in tobacco and heterologous expression in *E. coli*. Interestingly, during *MdPSY2* amplification and sequencing, two representative polymorphic variants (*MdPSY2_F* and *MdPSY2_CG*; Fig. 5) were obtained in five of eight sequenced clones. *Md*PSY2_F and *Md*PSY2_CG as well as *Md*PSY2 and *Md*PSY5 contain the trans-isoprenyl pyrophosphate synthase family functional domain and the Mg^{2+} substrate binding site (Fig. 5), suggesting functionality *in vivo*. Nevertheless, the polymorphic *Md*PSY2_F and *Md*PSY2_CG variants possess a substitution to thymine at position 1061 (1061A > T) producing the mutation Y358 F in the C-terminal region. It is important to mention that the mutation Y358 F is present in the *M. domestica* genome (Chr09:11502429..11504902) and that Tyr358 is highly conserved among PSY enzymes belonging to monocots and dicots, as well as bacterial PSY orthologs such as *Alicyclobacillus acidocaldarius* PSY (PDB_{id} 4HD1) and *Staphylococcus aureus* PSY (PDB_{id} 2ZCO) (Fig.5). *MdPSY2_CG* also contains the deletion of 18 bp between the base pair 92 and 109 and a mutation at nucleotide position 121 G > A producing a change of Gly to Ser in the predicted signal peptide region (Fig. 5). At this point we decided to include the polymorphic variants to investigate the subcellular localisation of the predicted *Md*PSYs by using *Md*PSYs:GFP fusion proteins (Fig. 6). *Md*PSY5 showed a clear plastid localisation (Fig. 6d–f) as did *Md*PSY2, its variants (*Md*PSY2_F and *Md*PSY2_CG), and the positive control *At*DXR (Fig. 6a–c and Fig. 6g–o). However, GFP signal in the cytoplasmic membrane was also observed for *Md*PSY2, *Md*PSY2_F and *Md*PSY2_CG but not in the positive control, suggesting a double localisation to plastids and the cytoplasmic membrane for these three forms (Fig. 6g–o).

Following up these results, we determined the enzymatic activity of the *Md*PSYs. To do so, we used two previously published *E. coli* strains: BL21 pDS1B, engineered to produce β-carotene (orange phenotype) and BL-21 pDS1BΔcrtB that presents a white phenotype due to the lack of coloured carotenoids (Niklitschek et al., 2008) (Table S6). BL21 pDS1BΔcrtB was transformed with pET28a vectors carrying different versions of the *MdPSY* genes (Table S6). All the strains showed a similar growth profile and PSY protein amount (Fig. S2). In addition, the strains recovered the ability to produce β-carotene as observed in the yellow-orange colour of the pellet (Fig. 7a), suggesting functionality for all analysed protein versions. Interestingly, the *E. coli* strain complemented with the *MdPSY2* and *MdPSY5* genes produced around 57 mg/g dry weight of total carotenoids, while the strains complemented with *MdPSY2*_F or *MdPSY2*_CG produced only half that amount (Fig. 7b). This is consistent with the change in colour observed in the pellet which is more intense in the pDS1B control (196 mg/g of dry weight) followed by the strains complemented with *MdPSY2* and *MdPSY5*, and lastly by the two *MdPSY2*_F and *MdPSY2*_CG variants (Fig. 7a). Chromatograms obtained by Reverse Phase HPLC (RP-HPLC) showed a single peak in all the *Md*PSY complemented strains with a retention time between 40 and 42.5 min and with an absorption spectrum that corresponds to β-carotene (Fig. 7c). These results suggest that although all the evaluated *Md*PSY enzymes present a plastid localisation and are functionally active, *MdPSY2* and *MdPSY5* catalyse the conversion of phytoene in a more efficient manner than the *MdPSY2*_F and *MdPSY2*_CG polymorphic variants.

3.3. D modelling of MdPSY2 and MdPSY5 proteins from Malus domestica cv. 'Fuji'

Since point mutations in main domains/motifs of PSY proteins have been reported to affect protein activity (Arango et al., 2010; Fu et al., 2010; Shumskaya et al., 2012; Welsch et al., 2010), we modelled the 3D structure of the mature *Md*PSY2, *Md*PSY2_F and *Md*PSY5 proteins to determine whether the Tyr358Phe mutation could be responsible for the lower enzymatic activity. We decided to exclude the *Md*PSY2_CG polymorphic version because it is identical to *Md*PSY2_F in the mature protein sequence; the deletion exists in the predicted transit peptide region which is not part of the mature functional enzyme. For this purpose, the crystallised structures of available bacterial and *Homo sapiens* PSYs (named as squalene synthase) in the PDB database were used as templates. Using the MODELLER software, 10 different model structures were generated for each target sequence. The structures were refined using the 3Drefine and KoBaMIN servers, resulting in 50 structures that were evaluated with the Modfold4 server according to their scores (Fig. S3). In general, these structures showed a well evaluated profile except for the last ~40 residues (Fig. S3B). This is reflected in the B factor value (Fig. S4A), possibly due to a lack of coverage in this region in the templates used for modelling (4HD1, 2ZCO and 3VJ8). The verify3D score profile obtained for these models

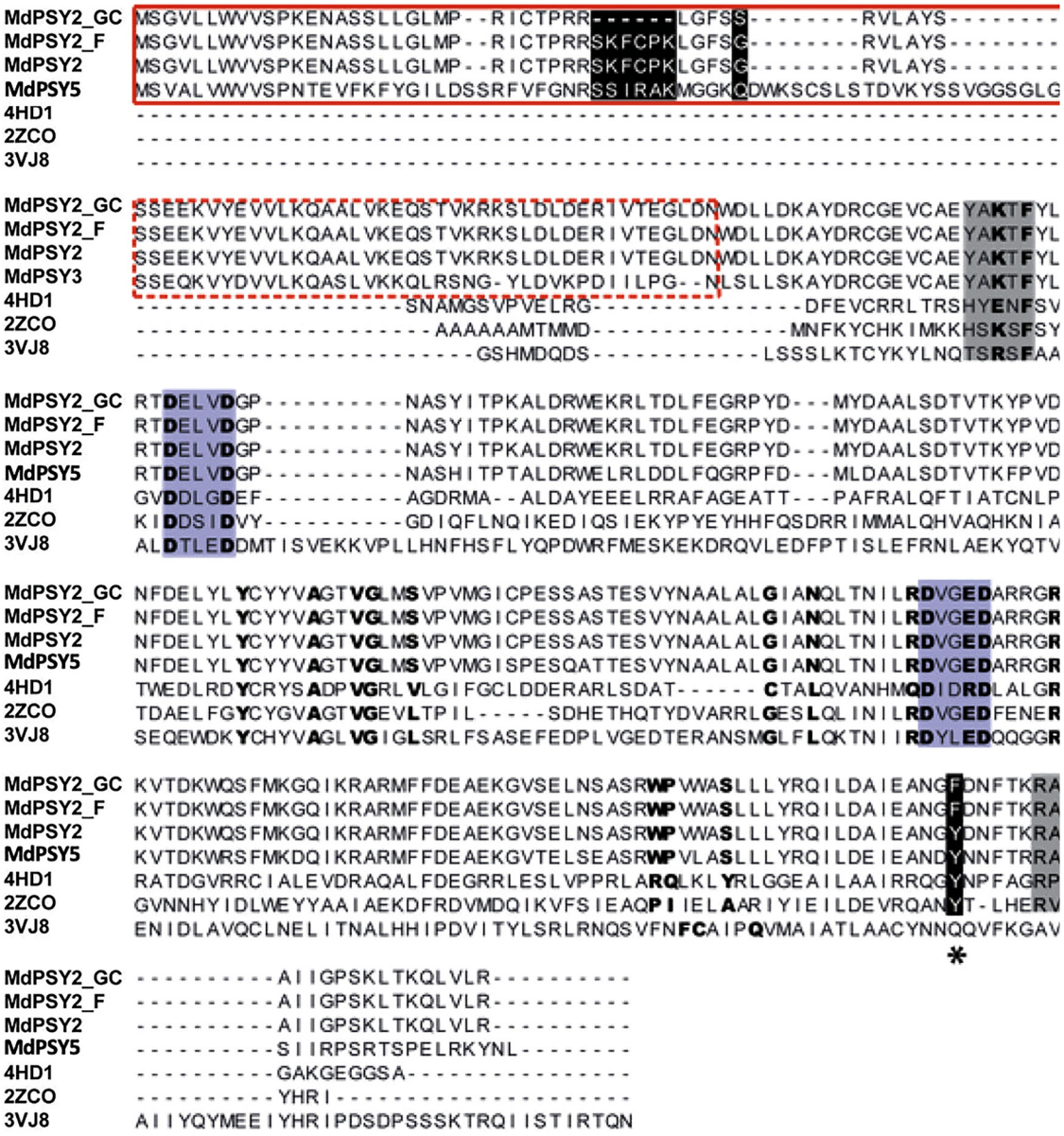

Fig. 5. Comparative alignment of *Md*PSY family members. For alignment, all *Md*PSY variants were included, as well as bacterial squalene synthase 4HD1 from *Alicyclobacillus acidocaldarius*, dehydro squalene synthase 2ZCO from *Staphylococcus aureus* and the *Homo sapiens* squalene synthase, 3VJ8. The predicted signal peptide is highlighted with a red rectangle and the region which has no homology with bacterial orthologues is punctuated in red. Black rectangles show the six amino acids deletion in the signal peptide of *Md*PSY2_GC and the change of Gly to Ser. The grey rectangle with bold letters shows the functional domain of the trans-isoprenyl pyrophosphate synthase family (TIPPSHH). Blue rectangles show the site for Mg^{2+} binding. The Y358F substitution at the C-terminal region in *Md*PSY2_CG and *Md*PSY2_F is highlighted in bold and with an asterisk. The grey rectangle at the C-terminal highlights the lid at the active site. The amino acids of the catalytic site and for substrate binding are highlighted in bold. The alignment was created using ClustalW. (For interpretation of the references to colour in this figure legend, the reader is referred to the web version of this article.)

showed that all the functional regions scored above 0.2, which is the lower threshold in this analysis (Fig. S4B). However, the region around the Tyr358Phe (C-terminal region) and the lid of the active site were below this threshold mainly because they are located in a low coverage region, as explained above. According to the analysis, three final models were chosen (Fig. 8a). Regarding the overall structure of the models, it was possible to find 14 (*Md*PSY2) or 15 (*Md*PSY2_F and *Md*PSY5) alpha helices. Five of these alpha helices (2, 3, 7, 8 and 12) form a central cavity which probably binds to the substrate (Fig. 8B). In addition, these five helices contain the residues comprising the catalytic site and the substrate binding site (Fig. 8b). In the external side of the central cavity it is possible to find the regions that maintain the intermediary pre-phytoene diphosphate (PPPP; Fig. 1) isolated from the solvent (as a lid over the active site) and the aspartate-rich motif (Fig. 8b). These regions can bind the substrate-Mg^{2+} complex and carry out the first step to produce PPPP. The curl in which Tyr358Phe is located, includes one of the two sites involved in the entrance to the active site. These regions are involved in the first reaction for the synthesis and stabilisation of the pre-phytoene intermediary, preventing water molecules interacting with it (Pandit et al., 2000, 2002). This result allows us to propose that the Tyr358Phe mutation in *Md*PSY2_F and *Md*PSY2_CG possibly affects electrostatic interactions with residues in the vicinity of the active site, and could explain the lower enzymatic activity obtained for *Md*PSY2_F and *Md*PSY2_CG in the *E. coli* complementation assay.

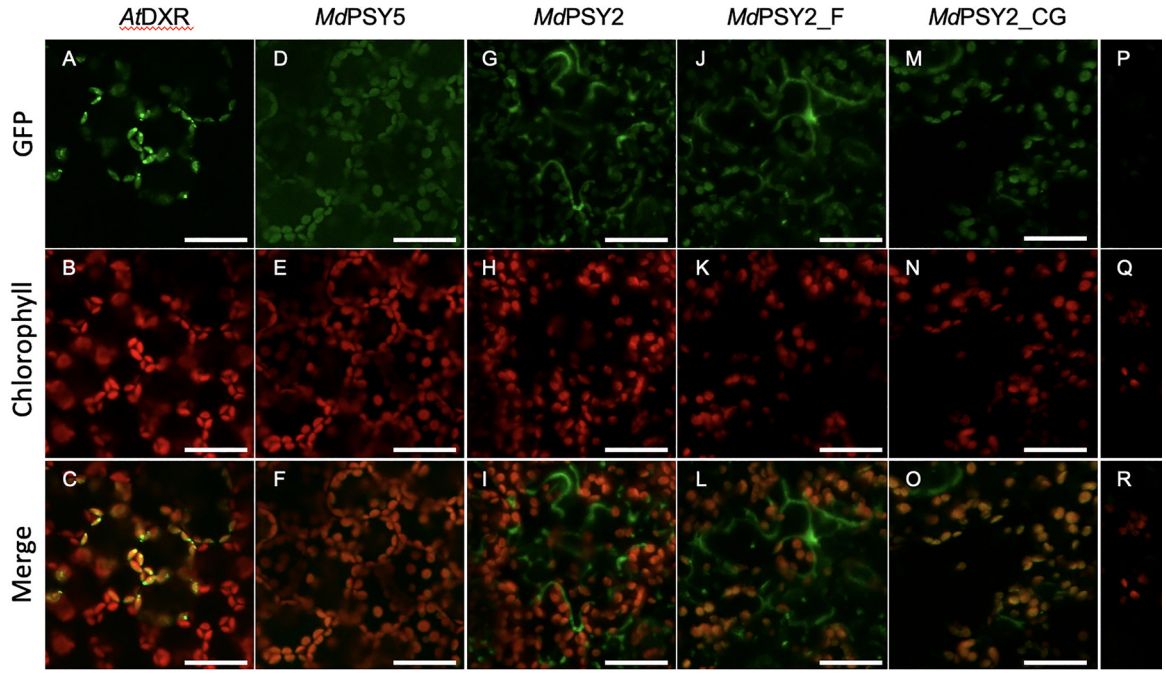

Fig. 6. Subcellular localisation of *Md*PSY5, *Md*PSY2, *Md*PSY2F and *Md*PSY2GC. Leaves of tobacco plants were agroinfiltrated with *A. tumefaciens* carrying 35S::*At*DXR (positive control, A-C), 35S::*Md*PSY5 (D-F), 35S::*Md*PSY2 (G-I), 35S::*Md*PSY2-F (F-L), *Md*PSY2-CG (M-O), without infiltration (negative control, P-R) and 35S::*At*PAR1 (nuclear control, S-U). Epidermal peels were observed by confocal microscopy 6 days after infiltration. All images were taken with 40x augmentation and GFP fluorescence was observed after excitation at 488 nm. Scale bar = 20 μM.

4. Discussion

There is a growing interest in the generation of new plant varieties with higher carotenoid content (Alos et al., 2016; Bhullar and Gruissem, 2013; Welsch et al., 2010). Due to the worldwide popularity of apples, they are an excellent candidate for carotenoid metabolic engineering. Apple fruits have a very low natural carotenoid content which could be the result of deficient synthesis, deficient stabilisation and/or an efficient degradation process. Considering that PSY is the key regulatory point of carotenoid synthesis, the aim of this study was to analyse the functionality of *MdPSY* family members in order to determine whether the functionality of this enzyme is responsible for the low carotenoid content in the flesh of apple fruits.

The apple genome has twelve predicted *MdPSY* genes (Velasco et al., 2010) but only four of them have available transcript data in the EST expression library derived from the GDR database (Text S1 and S2). The presence of multiple *PSY* genes is very common in plants; however, other plants have smaller PSY families with specific functions (Fraser et al., 2002; Li et al., 2008; Welsch et al., 2008). The predicted PSY proteins show over 68% sequence identity with previously reported PSY enzymes (Table S1), including the conserved domain rich in aspartate and the amino acids in the active site (Fig. S1). The high similarity between *Md*PSY sequences is probably due to a suggested genetic duplication event which was evidenced during *M. domestica* genome assembly (Velasco et al., 2010). Moreover, some genomic regions are repeated six times, which suggests that *M. domestica* has a hexaploid ancestor (Giovannoni, 2010). A phylogenetic tree showed that *Md*PSY3 grouped far away from the other three *Md*PSYs, which may be related to 13 amino acids that are absent in the other PSYs. These additional amino acids are located between the first motif of the active site and the aspartate-rich motif (Fig. S1) which could confer reduced functionality on this protein, in comparison with other reported PSY enzymes (Table S1). Additionally, *Md*PSY3 belongs to a more-recently conserved and widespread clade, exclusively formed by dicots, that could be involved in nutrient stress tolerance and mycorrhisation (Walter et al., 2015). The expression of *MdPSY3* under such specific conditions may have influenced the low representativeness in the EST databases used in our work. On the other hand, *Md*PSY5 is grouped in a clade with *At*PSY, *Sl*PSY1 and *Sl*PSY2, with proven *in vivo* functionality (Ruiz-Sola and Rodriguez-Concepción, 2012; Fraser et al., 1999, 2002; Fray and Grierson, 1993). *At*PSY, the only phytoene synthase in Arabidopsis, has an indispensable role for carotenoid synthesis in the complete plant (Ruiz-Sola and Rodriguez-Concepcion, 2012). *SlPSY1* encodes a plastid-localised fruit-specific phytoene synthase (PSY1) (Fray and Grierson, 1993) and *Sl*PSY2, functions specifically in chloroplast-containing tissues (Fraser et al., 1999, 2002). Transgenic tomato plants with reduced levels of *SlPSY1* were impaired in carotenoid accumulation in ripe fruit without affecting pigment composition in leaves (Fantini et al., 2013; Fraser et al., 2002; Ray et al., 1992). *Md*PSY1 and *Md*PSY2 grouped in a clade with *Zm*PSY2 and *Os*PSY2 from maize and rice, respectively, which have been localised to plastidial speckles (Shumskaya et al., 2012) and are expressed in several plant tissues including leaves, roots and embryos (Li et al., 2008; Welsch et al., 2008). In Fuji apple, unlike *MdPSY1* and *MdPSY5*, *MdPSY2* and *MdPSY3* are preferably expressed in mature fruits compared to leaves; however, at the mature stage of fruit development (as well as in leaves), *MdPSY2* and *MdPSY5* are the most highly-expressed genes. The differential expression of *MdPSYs* forms in leaves and the flesh of fruits may constitute a regulatory mechanism governing carotenoid synthesis in chloroplast- and chromoplast-containing organs in apple. Unequal gene expression between paralogs is consistent with a previous study where *MdPSY2* showed higher transcript level in skin and flesh of Royal Gala and Granny Smith apple fruits, as well as in leaves, compared to *MdPSY1* (Ampomah-Dwamena et al., 2015). Interestingly, *MdPSY5* was not previously analysed by Ampomah-Dwamena et al. (2012, 2015) because there was no evidence for its expression in the apple EST libraries used at the time (Newcomb et al., 2006). Therefore, this work not only provides experimental evidence of *MdPSY5* expression using other EST databases, but also offers the first functional characterisation and modelling of this gene.

The fact that *MdPSY2* and *MdPSY5* expression levels are consistent with carotenoid abundance in mature Fuji fruits, suggests that they have a dominant role in this species and may be primarily responsible

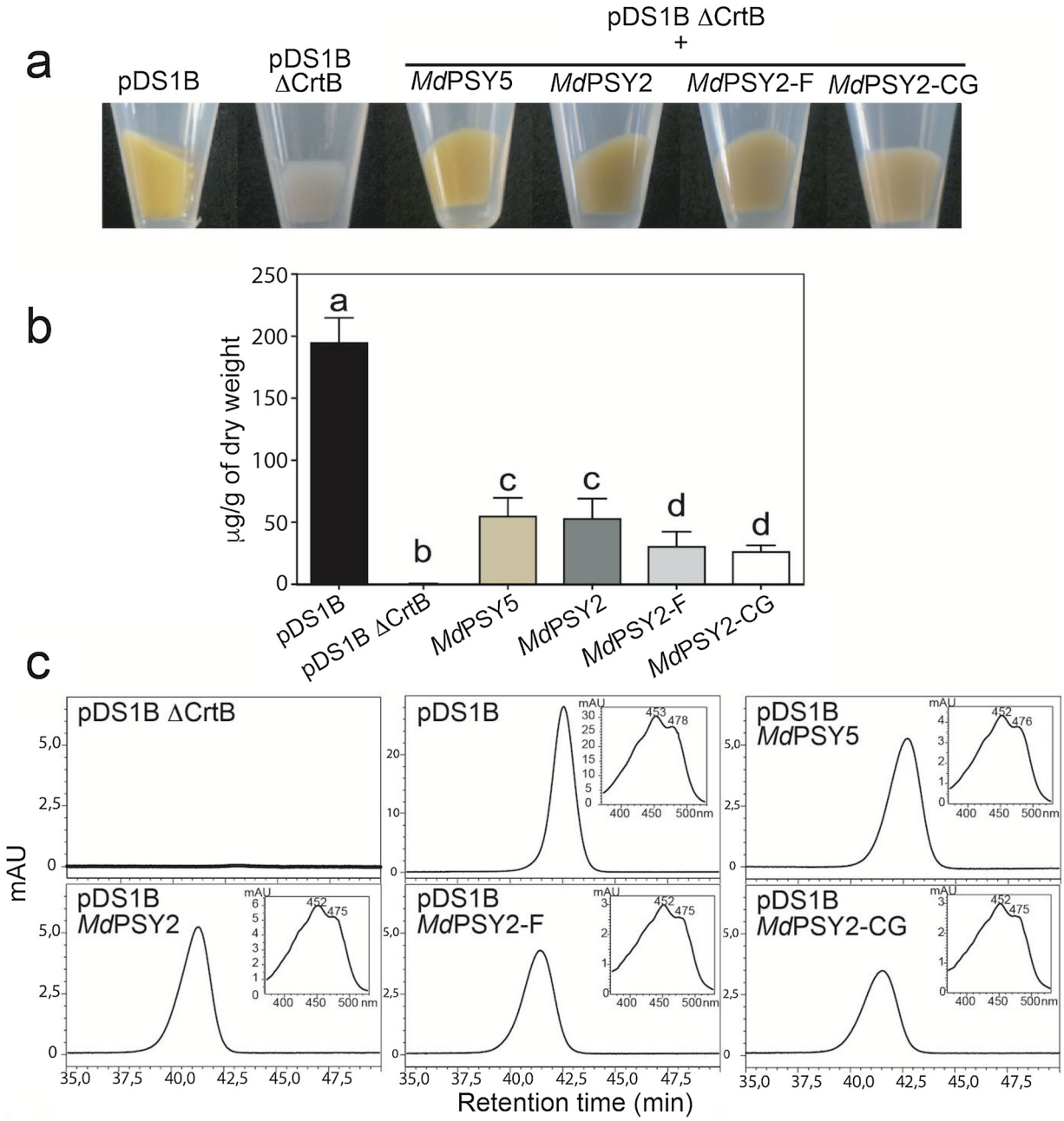

Fig. 7. Heterologous complementation of *E. coli* pDS1BΔcrtB strain with *MdPSY5*, *MdPSY2* and *MdPSY2* variants. (a) Bacteria phenotype of the pDS1B and pDS1BΔcrtB strains complemented with *MdPSY5*, *MdPSY2*, *MdPSY2_F* and *MdPSY2_CG*. (b) Total carotenoid quantification in the pDS1B and pDS1BΔcrtB strains complemented with *MdPSY5*, *MdPSY2*, *MdPSY2_F* and *MdPSY2_CG*. (c) Carotenoid composition of pigments produced by pDS1B and pDS1BΔcrtB strains complemented with *MdPSY5*, *MdPSY2*, *MdPSY2_F* and and *MdPSY2_CG*. Chromatograms for all the strains show a single peak corresponding to β-carotene. One-way ANOVA, $p < 0.0001$, was performed to determine differences among all the samples. Letters indicate significant differences between the samples.

for this first step in carotenoid synthesis compared to the other paralogs. Furthermore, the *MdPSY5* expression level correlates with carotenoid increments during fruit ripening. Previously, early pathway genes such as *MdPDS* and *MdCRTISO* were proposed as candidate genes to play a more important role in determining carotenoid abundance (Ampomah-Dwamena et al. 2012). In this work, *MdPDS*, *MdLCYB1* and *MdLCYB2* did not significantly change their expression during fruit ripening, although functional studies are required to exclude them from a regulatory role in apple carotenoid biosynthesis.

Proper carotenoid synthesis is influenced by the correct plastid localisation of the carotenogenic enzymes. The *Md*PSY2 and *Md*PSY5 proteins from Fuji apple localised to chloroplasts, although *Md*PSY2 as well as *Md*PSY2_F and *Md*PSY2_CG were also present in the cytoplasmic membrane (Figs. 5 and 6). *Md*PSY2_CG presented a six-amino-acid deletion in the transit peptide region which did not affect its predicted (Table S4) or experimentally-determined localisation in plastids (Fig. 6). Previously, *Md*PSY2:YFP was reported to localise in plastids in etiolated maize leaf protoplasts (Ampomah-Dwamena et al., 2012) and here, we provide further evidence for the proper plastidial localisation of the polymorphic variants. The reduced β-carotene production by the strain complemented with *Md*PSY2_F and *Md*PSY2_CG variants seems to be related to the mutation (Tyr358Phe) in the C-terminal region of the protein and not to the amount of total proteins in *E.coli* BL21 complemented *Md*PSYs strain or to the total amount of PSY (Fig. S2). Changes in the enzymatic activity due to point mutations have been previously reported for *Zm*PSY (Shumskaya et al., 2012; Welsch et al.,

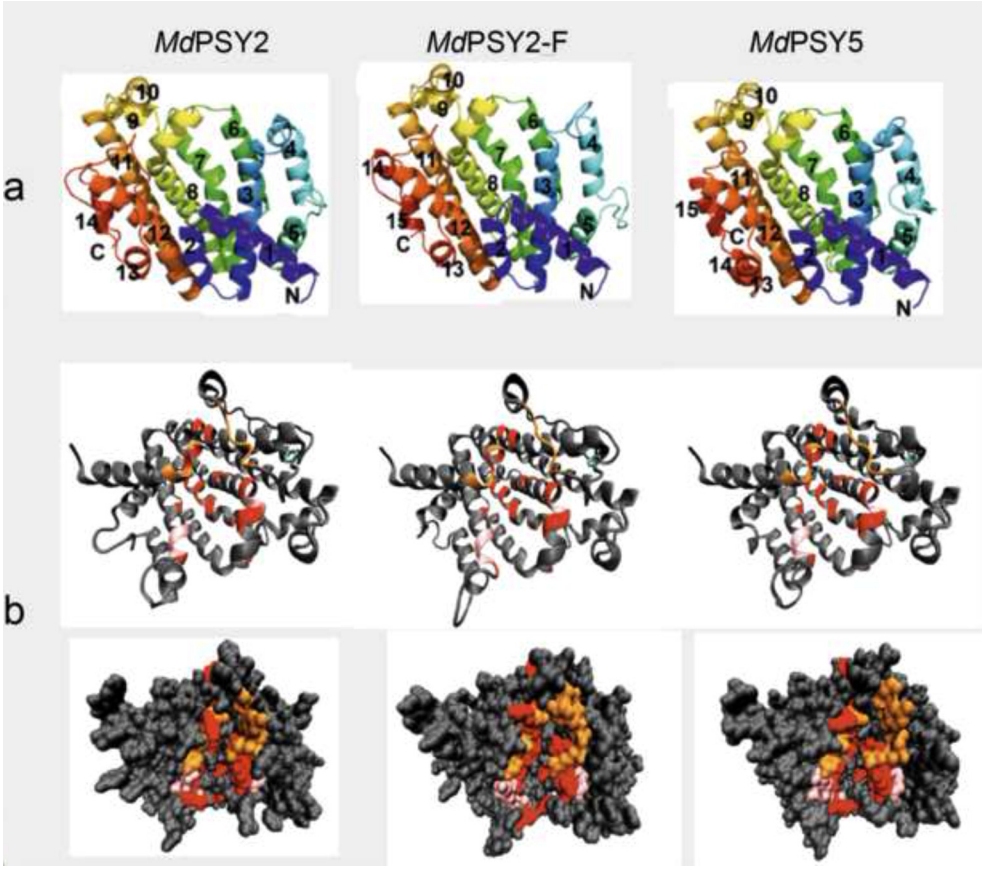

Fig. 8. Predicted models and functional regions of the *Md*PSY2, *Md*PSY2_F and *Md*PSY5 proteins. (a) Predicted models for *Md*PSY2, *Md*PSY2_F and *Md*PSY5. Amino-(N) and carboxy-(C) terminal sides are shown in bold face while the order of each alpha-helix is represented with a number (1-14/15). (b) Alpha-helix and representation of the surface of the enzyme. Residues from the catalytic site and substrate binding site (red), lid of the active site (orange), regions of substrate-Mg^{2+} binding (pink), Tyr358 residue (cyan; *Md*PSY2), Phe358 residue (cyan; *Md*PSY2_F) and Tyr386 residue (cyan; *Md*PSY5) are shown. (For interpretation of the references to colour in this figure legend, the reader is referred to the web version of this article.)

2010) and *Sl*PSY (Gady et al., 2012). In the case of loquat fruit, phytoene biosynthesis is carried out by *PSY1* in the peel and by *PSY2* in the flesh (Fu et al., 2014). A mutation in the C-terminal region of the PSY2A isoform is responsible for the lack of carotenoids in the flesh of white loquat varieties. Moreover, another isoform (PSY2B) appears to be responsible for carotenoid biosynthesis in loquat leaves (Fu et al., 2014), demonstrating a highly specialised tissue-specific regulation of carotenoid synthesis. Similar evidence has been reported for PSY of maize and cassava (Arango et al., 2010; Shumskaya et al., 2012). In this work, *3D*- modelling (Sharma et al., 2010; Shumskaya et al., 2012) of *Md*PSY2, *Md*PSY2_F and *Md*PSY5 showed a region conformed by five α-helices that surrounds a central cavity where the substrate is likely to bind. These features are similar to those of other enzymes of the trans-isoprenyl diphosphate synthase family with known structures (Liu et al., 2008; Pandit et al., 2000). Although the Tyr358 amino acid does not interact directly with the substrate or with some of the conserved sites, the change of Tyr to an aromatic residue such as Phe, could affect the formation of hydrogen bonds with the proximal Glu354 (Fig. S4F–H), and favour the Van der Waals interactions with the hydrophobic cavity in the active site (Fig. S4B, C, D, E). In turn, these interactions could affect the mobility of the region involved in the stabilisation of the intermediary, decreasing enzymatic activity as observed in the *in vitro* experiments. Nevertheless, in order to understand how the change of this amino acid within the turn adjacent to the lid of the active site could affect the interaction between the enzyme and the substrate or the intermediary, additional approaches such as docking and molecular dynamics simulations must be performed.

It is important to reiterate that the content of carotenoids depends on their rate of synthesis, stabilisation and degradation (Ruiz-Sola and Rodriguez-Concepcion, 2012). Therefore, the stability and activity of the *Md*PSY protein (given by the OR chaperone) could be the rate limiting step in carotenogenesis in apple (Zhou et al., 2015). In addition, OR induces chromoplast differentiation (Chayut et al., 2017; Lu et al., 2006) and genetic studies in melon revealed its role in stabilizing PSY and inhibiting β-carotene turnover (Chayut et al., 2017). Recently, the presence of the Or gene was genetically associated with carotenoid synthesis in coloured carrot varieties (Ellison et al., 2018) which could be a promising approach to carry out in apples. However, the improvement in sink capacity cannot be achieved without an adequate biosynthesis (Sun et al., 2018). Another possibility is that carotenoids in apple fruits are degraded to apocarotenoids by carotenoid cleavage dioxygenases (CCDs) (Beltran and Stange, 2016; Brandi et al., 2011; Lado et al., 2016). For instance, in chrysanthemum, all the white-flowered cultivars presented high levels of *CmCCD4a* transcripts and the suppression of the expression of this gene by RNAi increased carotenoid accumulation in petals (Ohmiya et al., 2006). In addition, white peach lines have functional CCD4 and a nonfunctional *ccd4* mutant was found in yellow-flesh peaches, suggesting that this enzyme is involved in colouration of the flesh in peach fruits (Fukamatsu et al., 2013). By an *in vivo E. coli* heterologous complementation assay, *Md*CCD4 isolated from *M. domestica* was able to cleave β-carotene to yield β-ionone (Huang et al., 2009). In addition, CCD1 expression at the ripe fruit stage was high in the β-carotene-rich 'Aotea' genotype and low in carotenoid-poor genotypes like 'Granny Smith' and 'M. 9′ (Ampomah-Dwamena et al., 2012). Considering that β-carotene is the main substrate for CCDs, this evidence suggests that this enzyme is not involved in removing this compound. These findings highlight the complexity of carotenoid regulation in apples and more evidence is required on the regulatory role of enzymes involved in the synthesis and degradation of carotenoids to explain the low accumulation of these pigments in apple fruits.

In summary, here we present evidence showing the functionality of four different *MdPSY* genes, *MdPSY2* and *MdPSY5* and the polymorphic *MdPSY2*_F and *MdPSY2*_CG variants. Taken together, the high *MdPSY2* and *MdPSY5* expression levels (in leaf and during fruit ripening), their plastid localisation, a proper tertiary structure, and the ability to

produce β-carotene in a heterologous *in vivo* system, lead us to suggest the *in vivo* functionality of both genes in apple flesh. The presence of polymorphic *Md*PSY2 mutants with lower activity could partially account for the lower carotenoid content, which may be compensated by the presence of fully functional *Md*PSY5 and *Md*PSY2 enzymes in the flesh of Fuji apples. If so, PSY activity would not be the limiting factor for the low carotenoid abundance in apple 'Fuji' Raku Raku. Future work to unveil the underlying mechanisms that explain low carotenoid abundance in *M. domestica* cv. 'Fuji' Raku Raku fruits should be focused on the functional characterisation of other genes involved in carotenoid synthesis (*e.g. MdPDS* or *MdLCYB*), in proteins involved in carotenoid stabilisation and accumulation (such as OR) or enzymes for carotenoid degradation (*e.g.* CCDs) which cause depletion of the carotenoid pool.

Author contribution statement

AC: performed *in silico* analysis, carotenoid quantification and expression analysis, JCM: prepared the figures and wrote the manuscript with CS, DA: carried out the heterologous complementation, FG performed the subcellular localisation, JCC and RC: performed in silico modelling, CS: designed experiments and wrote the manuscript.

Declaration of Competing Interest

The author(s) declare no competing interests.

Acknowledgements

This work was financed by the Chilean CONICYT funding (Fondecyt 1130245 and 1180747 and, FONDEF D10I1022) and the ENL005/2017 grant form the University of Chile. We thank Dr Monika Chodasiewicz for helpful comments throughout the manuscript and Dr Michael Handford (Universidad de Chile) for language support.

Appendix A. Supplementary data

Supplementary material related to this article can be found, in the online version, at doi:https://doi.org/10.1016/j.jplph.2020.153166.

References

Alos, E., Rodrigo, M.J., Zacarias, L., 2016. Manipulation of carotenoid content in plants to improve human health. Subcell. Biochem. 79, 311–343.
Alquezar, B., Zacarias, L., Rodrigo, M.J., 2009. Molecular and functional characterization of a novel chromoplast-specific lycopene beta-cyclase from citrus and its relation to lycopene accumulation. J. Exp. Bot. 60, 1783–1797.
Ampomah-Dwamena, C., Dejnoprat, S., Lewis, D., Sutherland, P., Volz, R.K., Allan, A.C., 2012. Metabolic and gene expression analysis of apple (Malus x domestica) carotenogenesis. J. Exp. Bot. 63 (12), 4497–4511.
Ampomah-Dwamena, C., Driedonks, N., Lewis, D., Shumskaya, M., Chen, X., Wurtzel, E.T., Espley, R.V., Allan, A.C., 2015. The Phytoene synthase gene family of apple (Malus x domestica) and its role in controlling fruit carotenoid content. BMC Plant Biol. 15, 185.
Andersen, C.L., Jensen, J.L., Orntoft, T.F., 2004. Normalization of real-time quantitative reverse transcription-PCR data: a model-based variance estimation approach to identify genes suited for normalization, applied to bladder and colon cancer data sets. Cancer Res. 64 (15), 5245–5250.
Arango, J., Wust, F., Beyer, P., Welsch, R., 2010. Characterization of phytoene synthases from cassava and their involvement in abiotic stress-mediated responses. Planta 232 (5), 1251–1262.
Beltran, J.C.M., Stange, C., 2016. Apocarotenoids: a new carotenoid-derived pathway. Subcell. Biochem. 79, 239–272.
Bhullar, N.K., Gruissem, W., 2013. Nutritional enhancement of rice for human health: the contribution of biotechnology. Biotechnol. Adv. 31 (1), 50–57.
Bou-Torrent, J., Toledo-Ortiz, G., Ortiz-Alcaide, M., Cifuentes-Esquivel, N., Halliday, K.J., Martinez-Garcia, J.F., Rodriguez-Concepcion, M., 2015. Regulation of carotenoid biosynthesis by shade relies on specific subsets of antagonistic transcription factors and co-factors. Plant Physiol. 169, 1584–1594.
Brandi, F., Bar, E., Mourgues, F., Horvath, G., Turcsi, E., Giuliano, G., Liverani, A., Tartarini, S., Lewinsohn, E., Rosati, C., 2011. Study of' Redhaven' peach and its white-fleshed mutant suggests a key role of CCD4 carotenoid dioxygenase in carotenoid and norisoprenoid volatile metabolism. BMC Plant Biol. 11, 24.
Carretero-Paulet, L., Ahumada, I., Cunillera, N., Rodríguez-Concepción, M., Ferrer, A., Boronat, A., et al., 2002. Expression and molecular analysis of the Arabidopsis DXR gene encoding 1-deoxy-D-xylulose 5-phosphate reductoisomerase, the first committed enzyme of the 2-C-methyl-Derythritol 4-phosphate pathway. Plant Physiol. 129, 1581–1591.
Chayut, N., Yuan, H., Ohali, S., Meir, A., Sa'ar, U., Tzuri, G., Zheng, Y., Mazourek, M., Gepstein, S., Zhou, X., Portnoy, V., Lewinsohn, E., Schaffer, A.A., Katzir, N., Fei, Z., Welsch, R., Li, L., Burger, J., Tadmor, Y., 2017. Distinct mechanisms of the ORANGE protein in controlling carotenoid flux. Plant Physiol. 173 (1), 376–389.
Cunningham Jr., F.X., Pogson, B., Sun, Z., McDonald, K.A., DellaPenna, D., Gantt, E., 1996. Functional analysis of the beta and epsilon lycopene cyclase enzymes of Arabidopsis reveals a mechanism for control of cyclic carotenoid formation. Plant Cell 8, 1613–1626.
Curtis, M.D., Grossniklaus, U., 2003. A gateway cloning vector set for high-throughput functional analysis of genes in planta. Plant Physiol. 133, 462–469.
Ellison, S.L., Luby, C.H., Corak, K.E., Coe, K.M., Senalik, D., Iorizzo, M., Goldman, I.L., Simon, P.W., Dawson, J.C., 2018. Carotenoid presence is associated with the or gene in domesticated carrot. Genetics 210 (4), 1497–1508.
Fantini, E., Falcone, G., Frusciante, S., Giliberto, L., Giuliano, G., 2013. Dissection of tomato lycopene biosynthesis through virus-induced gene silencing. Plant Physiol. 163 (2), 986–998.
Fraser, P.D., Bramley, P.M., 2004. The biosynthesis and nutritional uses of carotenoids. Prog. Lipid Res. 43 (3), 228–265.
Fraser, P.D., Kiano, J.W., Truesdale, M.R., Schuch, W., Bramley, P.M., 1999. Phytoene synthase-2 enzyme activity in tomato does not contribute to carotenoid synthesis in ripening fruit. Plant Mol. Biol. 40 (4), 687–698.
Fraser, P.D., Schuch, W., Bramley, P.M., 2000. Phytoene synthase from tomato (Lycopersicon esculentum) chloroplasts – partial purification and biochemical properties. Planta 211 (3), 361–369.
Fraser, P.D., Romer, S., Shipton, C.A., Mills, P.B., Kiano, J.W., Misawa, N., Drake, R.G., Schuch, W., Bramley, P.M., 2002. Evaluation of transgenic tomato plants expressing an additional phytoene synthase in a fruit-specific manner. Proc. Natl. Acad. Sci. U. S. A. 99 (2), 1092–1097.
Fray, R.G., Grierson, D., 1993. Identification and genetic analysis of normal and mutant phytoene synthase genes of tomato by sequencing, complementation and co-suppression. Plant Mol. Biol. 22 (4), 589–602.
Fu, Z., Yan, J., Zheng, Y., Warburton, M.L., Crouch, J.H., Li, J.S., 2010. Nucleotide diversity and molecular evolution of the PSY1 gene in Zea mays compared to some other grass species. Theor. Appl. Genet. 120 (4), 709–720.
Fu, X., Feng, C., Wang, C., Yin, X., Lu, P., Grierson, D., Xu, C., Chen, K., 2014. Involvement of multiple phytoene synthase genes in tissue- and cultivar-specific accumulation of carotenoids in loquat. J. Exp. Bot. 65 (16), 4679–4689.
Fuentes, P., Pizarro, L., Moreno, J.C., Handford, M., Rodriguez-Concepcion, M., Stange, C., 2012. Light-dependent changes in plastid differentiation influence carotenoid gene expression and accumulation in carrot roots. Plant Mol. Biol. 79 (1-2), 47–59.
Fukamatsu, Y., Tamura, T., Hihara, S., Oda, K., 2013. Mutations in the CCD4 carotenoid cleavage dioxygenase gene of yellow-flesh peaches. Biosci. Biotechnol. Biochem. 77 (12), 2514–2516.
Gady, A.L., Vriezen, W.H., Van de Wal, M.H., Huang, P., Bovy, A.G., Visser, R.G., Bachem, C.W., 2012. Induced point mutations in the phytoene synthase 1 gene cause differences in carotenoid content during tomato fruit ripening. Mol. Breed. 29 (3), 801–812.
Giovannoni, J., 2001. Molecular biology of fruit maturation and ripening. Annu. Rev. Plant Physiol. Plant Mol. Biol. 52, 725–749.
Giovannoni, J., 2010. Harvesting the apple genome. Nat. Genet. 42 (10), 822–823.
Gu, P., Ishii, Y., Spencer, T.A., Shechter, I., 1998. Function-structure studies and identification of three enzyme domains involved in the catalytic activity in rat hepatic squalene synthase. J. Biol. Chem. 273, 12515–12525.
Guzman, I., Hamby, S., Romero, J., Bosland, P.W., O'Connell, M.A., 2010. Variability of carotenoid biosynthesis in orange colored Capsicum spp. Plant Sci. 179 (1–2), 49–59.
Hirschberg, J., 2001. Carotenoid biosynthesis in flowering plants. Curr. Opin. Plant Biol. 4 (3), 210–218.
Huang, F.C., Molnar, P., Schwab, W., 2009. Cloning and functional characterization of carotenoid cleavage dioxygenase 4 genes. J. Exp. Bot. 60 (11), 3011–3022.
Humphrey, W., Dalke, A., Schulten, K., 1996. VMD: visual molecular dynamics. J. Mol. Graph. 14, 33–38.
Just, B.J., Santos, C.A., Fonseca, M.E., Boiteux, L.S., Oloizia, B.B., Simon, P.W., 2007. Carotenoid biosynthesis structural genes in carrot (Daucus carota): isolation, sequence-characterization, single nucleotide polymorphism (SNP) markers and genome mapping. Theor. Appl. Genet. 114 (4), 693–704.
Kato, M., Ikoma, Y., Matsumoto, H., Sugiura, M., Hyodo, H., Yano, M., 2004. Accumulation of carotenoids and expression of carotenoid biosynthetic genes during maturation in citrus fruit. Plant Physiol. 134 (2), 824–837.
Kromdijk, J., Glowacka, K., Leonelli, L., Gabilly, S.T., Iwai, M., Niyogi, K.K., Long, S.P., 2016. Improving photosynthesis and crop productivity by accelerating recovery from photoprotection. Science 354 (6314), 857–861.
Kumar, C.G., LeDuc, R., Gong, G., Roinishivili, L., Lewin, H.A., Liu, L., 2004. ESTIMA, a tool for EST management in a multi-project environment. BMC Bioinform. 5, 176.
Kumar, S., Stecher, G., Li, M., Knyaz, C., Tamura, K., 2018. MEGA X: molecular evolutionary genetics analysis across computing platforms. Mol. Biol. Evol. 35, 1547–1549.
Lado, J., Zacarias, L., Rodrigo, M.J., 2016. Regulation of carotenoid biosynthesis during fruit development. Subcell. Biochem. 79, 161–198.
Li, F., Vallabhaneni, R., Yu, J., Rocheford, T., Wurtzel, E.T., 2008. The maize phytoene synthase gene family: overlapping roles for carotenogenesis in endosperm, photomorphogenesis, and thermal stress tolerance. Plant Physiol. 147 (3), 1334–1346.
Li, L., Yuan, H., Zeng, Y., Xu, Q., 2016. Plastids and carotenoid accumulation. Subcell. Biochem. 79, 273–293.

Lichtenthaler, H.K., Buschmann, C., 2001. Chlorophylls and carotenoids: measurement and characterization by UV-VIS spectroscopy. Curr. Protoc. Food Anal. Chem. 1, F4.3.1–F4.3.8.
Liu, C.I., Liu, G.Y., Song, Y., Yin, F., Hensler, M.E., Jeng, W.Y., Nizet, V., Wang, A.H., Oldfield, E., 2008. A cholesterol biosynthesis inhibitor blocks Staphylococcus aureus virulence. Science 319 (5868), 1391–1394.
Lois, L.M., Rodriguez-Concepcion, M., Gallego, F., Campos, N., Boronat, A., 2000. Carotenoid biosynthesis during tomato fruit development: regulatory role of 1-deoxy-D-xylulose 5-phosphate synthase. Plant J. 22 (6), 503–513.
Lu, S., Van Eck, J., Zhou, X., Lopez, A.B., O'Halloran, D.M., Cosman, K.M., Conlin, B.J., Paolillo, D.J., Garvin, D.F., Vrebalov, J., Kochian, L.V., Kupper, H., Earle, E.D., Cao, J., Li, L., 2006. The cauliflower or gene encodes a DnaJ cysteine-rich domain-containing protein that mediates high levels of beta-carotene accumulation. Plant Cell 18 (12), 3594–3605.
Maass, D., Arango, J., Wust, F., Beyer, P., Welsch, R., 2009. Carotenoid crystal formation in Arabidopsis and carrot roots caused by increased phytoene synthase protein levels. PLoS One 4 (7), e6373.
Mann, V., Pecker, I., Hirschberg, J., 1994. Cloning and characterization of the gene for phytoene desaturase (Pds) from tomato (Lycopersicon esculentum). Plant Mol. Biol. 24 (3), 429–434.
Meisel, L., Fonseca, B., Gonzalez, S., Baeza-yates, R., cambiazo, V., Campos, R., Gonzalez, M., Orellana, A., Retamales, J., Silva, H., 2005. A rapid and efficient method for purifying high quality total RNA from peaches (Prunus persica) for functional genomics analyses. Biol. Res. 38, 83–88.
Moreno, J.C., Pizarro, L., Fuentes, P., Handford, M., Cifuentes, V., Stange, C., 2013. Levels of lycopene beta-cyclase 1 modulate carotenoid gene expression and accumulation in Daucus carota. PLoS One 8 (3), e58144.
Newcomb, R.D., Crowhurst, R.N., Gleave, A.P., Rikkerink, E.H., Allan, A.C., Beuning, L.L., Bowen, J.H., Gera, E., Jamieson, K.R., Janssen, B.J., Laing, W.A., McArtney, S., Nain, B., Ross, G.S., Snowden, K.C., Souleyre, E.J., Walton, E.F., Yauk, Y.K., 2006. Analyses of expressed sequence tags from apple. Plant Physiol. 141 (1), 147–166.
Niklitschek, M., Alcaino, J., Barahona, S., Sepulveda, D., Lozano, C., Carmona, M., Marcoleta, A., Martinez, C., Lodato, P., Baeza, M., Cifuentes, V., 2008. Genomic organization of the structural genes controlling the astaxanthin biosynthesis pathway of Xanthophyllomyces dendrorhous. Biol. Res. 41 (1), 93–108.
Nisar, N., Li, L., Lu, S., Khin, N.C., Pogson, B.J., 2015. Carotenoid metabolism in plants. Mol. Plant 8 (1), 68–82.
Ohmiya, A., Kishimoto, S., Aida, R., Yoshioka, S., Sumitomo, K., 2006. Carotenoid cleavage dioxygenase (CmCCD4a) contributes to white color formation in chrysanthemum petals. Plant Physiol. 142 (3), 1193–1201.
Pandit, J., Danley, D.E., Schulte, G.K., Mazzalupo, S., Pauly, T.A., Hayward, C.M., Hamanaka, E.S., Thompson, J.F., Harwood Jr., H.J., 2000. Crystal structure of human squalene synthase. A key enzyme in cholesterol biosynthesis. J. Biol. Chem. 275 (39), 30610–30617.
Pandit, S.B., Gosar, D., Abhiman, S., Sujatha, S., Dixit, S.S., Mhatre, N.S., Sowdhamini, R., Srinivasan, N., 2002. SUPFAM – a database of potential protein superfamily relationships derived by comparing sequence-based and structure-based families: implications for structural genomics and function annotation in genomes. Nucleic Acids Res. 30 (1), 289–293.
Pfaffl, M.W., 2001. A new mathematical model for relative quantification in real-time RT-PCR. Nucleic Acids Res. 29 (9), e45.
Qin, X., Coku, A., Inoue, K., Tian, L., 2011. Expression, subcellular localization, and cis-regulatory structure of duplicated phytoene synthase genes in melon (Cucumis melo L.). Planta 234 (4), 737–748.
Rao, A.V., Rao, L.G., 2007. Carotenoids and human health. Pharmacol. Res. 55 (3), 207–216.
Ray, J., Moureau, P., Bird, C., Bird, A., Grierson, D., Maunders, M., Truesdale, M., Bramley, P., Schuch, W., 1992. Cloning and characterization of a gene involved in phytoene synthesis from tomato. Plant Mol. Biol. 19 (3), 401–404.
Rodriguez-Suarez, C., Atienza, S.G., Piston, F., 2011. Allelic variation, alternative splicing and expression analysis of Psy1 gene in Hordeum chilense Roem. Et Schult. PLoS One 6 (5), e19885.
Rodriguez-Villalon, A., Gas, E., Rodriguez-Concepcion, M., 2009. Phytoene synthase activity controls the biosynthesis of carotenoids and the supply of their metabolic precursors in dark-grown Arabidopsis seedlings. Plant J. 60 (3), 424–435.
Ronen, G., Cohen, M., Zamir, D., Hirschberg, J., 1999. Regulation of carotenoid biosynthesis during tomato fruit development: expression of the gene for lycopene epsilon-cyclase is down-regulated during ripening and is elevated in the mutant Delta. Plant J. 17 (4), 341–351.
Ronen, G., Carmel-Goren, L., Zamir, D., Hirschberg, J., 2000. An alternative pathway to beta -carotene formation in plant chromoplasts discovered by map-based cloning of beta and old-gold color mutations in tomato. Proc Natl Acad Sci U S A 97, 11102–11107.
Rosas-Saavedra, C., Stange, C., 2016. Biosynthesis of carotenoids in plants: enzymes and color. Subcell. Biochem. 79, 35–69.
Ruiz-Sola, M.A., Rodriguez-Concepcion, M., 2012. Carotenoid biosynthesis in Arabidopsis: a colorful pathway. Arabidopsis book 10, e0158.
Schledz, M., al-Babili, S., von Lintig, J., Haubruck, H., Rabbani, S., Kleinig, H., Beyer, P., 1996. Phytoene synthase from Narcissus pseudonarcissus: functional expression, galactolipid requirement, topological distribution in chromoplasts and induction during flowering. Plant J. 10 (5), 781–792.
Sharma, M., Yi, M., Dong, H., Qin, H., Peterson, E., Busath, D.D., Zhou, H.X., Cross, T.A., 2010. Insight into the mechanism of the influenza A proton channel from a structure in a lipid bilayer. Science 330 (6003), 509–512.
Shumskaya, M., Bradbury, L.M., Monaco, R.R., Wurtzel, E.T., 2012. Plastid localization of the key carotenoid enzyme phytoene synthase is altered by isozyme, allelic variation, and activity. Plant Cell 24 (9), 3725–3741.
Sievers, F., Wilm, A., Dineen, D., Gibson, T.J., Karplus, K., Li, W., Lopez, R., McWilliam, H., Remmert, M., Soding, J., Thompson, J.D., Higgins, D.G., 2011. Fast, scalable generation of high-quality protein multiple sequence alignments using Clustal Omega. Mol. Syst. Biol. 7, 539.
Sun, T., Yuan, H., Cao, H., Yazdani, M., Tadmor, Y., Li, L., 2018. Carotenoid metabolism in plants: the role of plastids. Mol. Plant 11 (1), 58–74.
Tansey, T.R., Shechter, I., 2000. Structure and regulation of mammalian squalene synthase. Biochim. Biophys. Acta 1529, 49–62.
Tao, L., Yao, H., Cheng, Q., 2007. Genes from a Dietzia sp. For synthesis of C40 and C50 beta-cyclic carotenoids. Gene 386 (1–2), 90–97.
Velasco, R., et al., 2010. The genome of the domesticated apple (Malus x domestica Borkh.). Nat. Genet. 42 (10), 833–839.
von Lintig, J., Welsch, R., Bonk, M., Giuliano, G., Batschauer, A., Kleinig, H., 1997. Light-dependent regulation of carotenoid biosynthesis occurs at the level of phytoene synthase expression and is mediated by phytochrome in Sinapis alba and Arabidopsis thaliana seedlings. Plant J. 12 (3), 625–634.
Walter, M.H., Stauder, R., Tissier, A., 2015. Evolution of root-specificcarotenoid precursor pathways for apocarotenoid signal biogenesis. Plant Sci. 233, 1–10.
Waterhouse, A.M., Procter, J.B., Martin, D.M., Clamp, M., Barton, G.J., 2009. Jalview Version 2–a multiple sequence alignment editor and analysis workbench. Bioinformatics 25, 1189–1191.
Welsch, R., Beyer, P., Hugueney, P., Kleinig, H., von Lintig, J., 2000. Regulation and activation of phytoene synthase, a key enzyme in carotenoid biosynthesis, during photomorphogenesis. Planta 211 (6), 846–854.
Welsch, R., Wust, F., Bar, C., Al-Babili, S., Beyer, P., 2008. A third phytoene synthase is devoted to abiotic stress-induced abscisic acid formation in rice and defines functional diversification of phytoene synthase genes. Plant Physiol. 147 (1), 367–380.
Welsch, R., Arango, J., Bar, C., Salazar, B., Al-Babili, S., Beltran, J., Chavarriaga, P., Ceballos, H., Tohme, J., Beyer, P., 2010. Provitamin A accumulation in cassava (Manihot esculenta) roots driven by a single nucleotide polymorphism in a phytoene synthase gene. Plant Cell 22 (10), 3348–3356.
Zhou, X., Welsch, R., Yang, Y., Alvarez, D., Riediger, M., Yuan, H., Fish, T., Liu, J., Thannhauser, T.W., Li, L., 2015. Arabidopsis OR proteins are the major post-transcriptional regulators of phytoene synthase in controlling carotenoid biosynthesis. Proc. Natl. Acad. Sci. U. S. A. 112 (11), 3558–3563.